Archival Report

The Addiction-Susceptibility *TaqIA/Ankk1* Controls Reward and Metabolism Through D$_2$ Receptor-Expressing Neurons

Enrica Montalban, Roman Walle, Julien Castel, Anthony Ansoult, Rim Hassouna, Ewout Foppen, Xi Fang, Zach Hutelin, Sophie Mickus, Emily Perszyk, Anna Petitbon, Jérémy Berthelet, Fernando Rodrigues-Lima, Alberto Cebrian-Serrano, Giuseppe Gangarossa, Claire Martin, Pierre Trifilieff, Clémentine Bosch-Bouju, Dana M. Small, and Serge Luquet

ABSTRACT

BACKGROUND: A large body of evidence highlights the importance of genetic variants in the development of psychiatric and metabolic conditions. Among these, the TaqIA polymorphism is one of the most commonly studied in psychiatry. TaqIA is located in the gene that codes for the ankyrin repeat and kinase domain containing 1 kinase (Ankk1) near the dopamine D$_2$ receptor (D2R) gene. Homozygous expression of the A1 allele correlates with a 30% to 40% reduction of striatal D2R, a typical feature of addiction, overeating, and other psychiatric pathologies. The mechanisms by which the variant influences dopamine signaling and behavior are unknown.

METHODS: Here, we used transgenic and viral-mediated strategies to reveal the role of Ankk1 in the regulation of activity and functions of the striatum.

RESULTS: We found that *Ankk1* is preferentially enriched in striatal D2R-expressing neurons and that Ankk1 loss of function in the dorsal and ventral striatum leads to alteration in learning, impulsivity, and flexibility resembling endophenotypes described in A1 carriers. We also observed an unsuspected role of Ankk1 in striatal D2R-expressing neurons of the ventral striatum in the regulation of energy homeostasis and documented differential nutrient partitioning in humans with or without the A1 allele.

CONCLUSIONS: Overall, our data demonstrate that the Ankk1 gene is necessary for the integrity of striatal functions and reveal a new role for Ankk1 in the regulation of body metabolism.

https://doi.org/10.1016/j.biopsych.2023.02.010

Psychiatric diseases are multifactorial disorders, and the risk of developing these is influenced by both genetic and environmental factors. Even though classically considered as distinct pathologies, various psychiatric disorders share common symptomatic dimensions such as alterations of mood, cognitive functions, or reward processing, suggesting similar pathophysiological mechanisms. In line with this, the Research Domain Criteria classifies psychiatric illnesses based on common neurobiological, behavioral, or genetic dimensions, aimed at identifying both the mechanisms that are shared across multiple psychiatric disorders and the processes that are unique to specific psychiatric symptoms (1). Interestingly, psychiatric disorders are often accompanied by disturbances in energy metabolism and a higher risk of developing metabolic syndrome, with appetite changes as a core feature of multiple diseases (2). This raises the possibility of an overlap in the pathogenic mechanisms that underlie neuropsychiatric and metabolic symptoms.

It is well established that single nucleotide polymorphisms are associated with a higher risk of developing psychiatric disorders (3). Among single nucleotide polymorphisms, TaqIA

polymorphisms have attracted growing attention. The TaqIA polymorphism was initially believed to be in the D2R gene but was later mapped to the neighboring gene that codes for the ankyrin repeat and kinase domain containing 1 kinase (Ankk1) and corresponds to the single nucleotide polymorphism A2 (T→C) in the position 2137 of the *Ankk1* transcript (4). The TaqIA variant results in an amino acid change (E[GAG]→K [AAG], Glu→Lys) in position 713 of ANKK1 protein in humans. While the minor A1 variant is the ancestral polymorphism, the A2 variant has only recently appeared in primate evolution (5). Ankk1 maps onto chromosome 11 in humans and chromosome 9 in mice, which includes the dopamine receptor D$_2$ (D2R). TaqIA corresponds to 3 variants, A1/A1, A1/A2, and A2/A2. Approximately 30% of European, 80% of Asian, and 40% of African populations possess 1 or 2 copies of the A1 allele.

Strikingly, in humans, the A1 allele is associated with psychiatric and neurological disorders such as attention-deficit/hyperactivity disorder (6), Parkinson's disease (7), and addiction (8–10) as well as metabolic dysfunction and eating disorders (11–14). A1 carriers are more likely to have increased waist circumference and risk for obesity (14,15). Recent

studies have also reported an association between the presence of A1 and some of the characteristics of anorexia nervosa (13). Of note, weight loss has been reported to be easier in obese individuals bearing the A1 variant. Altogether, this suggests that A1 might be a genetic node for the convergence of neuropsychiatric and metabolic symptoms.

Alterations in reward processing, motivation, working memory, and cognitive flexibility, all characterized by dysregulation of the corticolimbic system and its regulation by dopamine neurotransmission (16,17), are observed across all the pathologies associated with TaqIA (15,18,19). Accordingly, the A1 variant is associated with reduced activity in the prefrontal cortex and striatum during reversal learning (15); reduced activity in the midbrain, prefrontal cortex, and thalamus during consumption of a milk shake (20); and greater impulsivity (15,21,22) or steeper delayed discounting, which are typical features of several psychiatric symptoms and eating disorders. Moreover, homozygous dosage of the A1 allele correlates with an ~30% to 40% reduction in striatal D2R abundance (23–25). Yet, such a decrease in D2R availability is a typical feature of addiction and is believed to be a core endophenotype responsible for compulsive drug consumption (26,27), overeating, and obesity-related reduction in activity (28).

These observations strongly suggest that 1) the interaction between environment and Ankk1 is critical in the susceptibility to reward-related and metabolic-based dysfunctions and 2) perturbations of various components of ingestive behavior in A1 carriers may result from a dysregulation of D2R-dependent dopamine transmission. To date, the molecular and cellular functions of Ankk1 remain largely unknown, primarily because of the lack of animal models. As a consequence, very little is known regarding the mechanisms by which A1 and A2 variants of Ankk1 alter dopamine signaling and, in general, in which direction those variants affect Ankk1 activity and D2R-related function to contribute to the protection or vulnerability to psychiatric and metabolic diseases.

METHODS AND MATERIALS

Animals

Both male and female Ankk1$^{lox/lox}$, Ankk1$^{\Delta\text{-}D2R\ Neurons}$ (Ankk1$^{\Delta\text{-}D2R\ N}$), and Drd2-Cre mice were used. Animal protocols were performed in accordance with the regulations and approved by the relevant committee: Paris, guidelines of the French Agriculture and Forestry Ministry for handling animals (decree 87–848) under the approval of the Direction Départementale de la Protection des Populations de Paris (authorization No. C-75-828, license B75-05-22), Animal Care Committee of the University of Paris (APAFIS No. 2015062611174320), Institut de Biologie Paris Seine of Sorbonne University (C75-05-24) (Supplemental Methods).

Human Participants

Thirty-six subjects were recruited from the greater New Haven, Connecticut, area, via flyers or social media advertisements. Subjects were enrolled in this pilot study based on body mass index (BMI) (<26) and underwent indirect calorimetry measurement and genotyping on separate days. All subjects provided written informed consent at the first visit, and the study

was approved by the Yale Human Investigation Committee (Supplemental Methods).

Total RNA Purification, Complementary DNA Preparation, and Real-Time Polymerase Chain Reaction

Real-time quantitative polymerase chain reaction (PCR) was normalized to a housekeeping gene using the delta-delta cycle threshold method (Supplemental Methods).

Pharmacological Treatments

For acute treatments, apomorphine (Tocris) was dissolved in phosphate-buffered saline and injected intraperitoneally (i.p.) (3 mg/kg). Phosphate-buffered saline was used as the vehicle treatment in control conditions. Haloperidol (Tocris) was dissolved in saline and injected i.p. (0.5 mg/kg).

Histology

Mice were anesthetized with pentobarbital (500 mg/kg, i.p.) (Sanofi-Aventis) and transcardially perfused with 4 °C paraformaldehyde (4%) for 5 minutes. Sections were processed as in (29) (Supplemental Methods).

Patch-Clamp Recordings of D2R Spiny Projection Neurons in the Nucleus Accumbens

Mice were anesthetized with isoflurane, decapitated, and coronal brain slice sections were prepared. D2R spiny projection neurons (SPNs) identified in the nucleus accumbens (NAc) were patch-clamped and recorded as described in Supplemental Methods.

Stereotaxic Injections

Ankk1$^{lox/lox}$ animals were anesthetized with isoflurane and received 10 mg/kg i.p. of Buprécare (buprenorphine 0.3 mg), diluted 1/100 in NaCl 9 g/L, and 10 mg/kg of Ketofen (ketoprofen 100 mg), diluted 1/100 in NaCl 9 g/L, and placed on a stereotactic frame (Model 940; David Kopf Instruments). We bilaterally injected 0.6 μL (dorsal striatum, DS) or 0.3 μL (NAc) of virus (AAV9.CMV.HI.eGFP-Cre.WPRE.SV40 or AAV5.CMV.HI.eGFP-Cre.WPRE.SV40) and GFP (green fluorescent protein) controls, (titer ≥ 10^{13} vg/mL, working dilution 1:10) into the DS (lateral = ±1.75; anteroposterior = +0.6; ventral = −3.5, and −3 in mm) or the NAc (lateral = ±1; anteroposterior = +1.55, ventral = −4.5) at a rate of 100 nL/min. The injection needle was carefully removed after 5 minutes waiting at the injection site and 2 minutes waiting halfway to the top.

Behavioral and Metabolic Characterization

Haloperidol-induced catalepsy was measured 45 to 180 minutes after haloperidol injection. The behavior of mice was explored using a food-cued T-maze paradigm, operant conditioning, and binge eating protocols (Supplemental Methods).

Binge Feeding Experiment

Intermittent access to a palatable food (High Fat Diet; ResearchDiet D12492i) was provided for 1 hour/day during 4 consecutive days from 10 to 11 AM. During binge sessions, chow pellets were not removed. The amount of the consumed palatable food was measured at the end of each session, and data were presented as kcal/body weight.

Metabolic Efficiency Analysis

All mice were monitored for metabolic efficiency (Labmaster; TSE Systems GmbH). After an initial period of acclimation of at least 2 days in the calorimetry cages, food and water intake, whole energy expenditure, oxygen consumption, carbon dioxide production, respiratory quotient (RQ) ($RQ = VCO_2/VO_2$, in which V is volume), and locomotor activity were recorded as previously described. Additionally, fatty acid oxidation was calculated as previously reported (30). Data are the result of the average of the last 3 days of recording. Before and after indirect calorimetry assessment, body mass composition was analyzed using an Echo Medical Systems EchoMRI (Whole Body Composition Analyzers; EchoMRI).

Statistical Analyses

Compiled data are reported as mean ± SEM with single data points plotted. Data were analyzed with GraphPad Prism 9. Normal distribution was tested with the Anderson-Darling, D'Agostino Pearson, Shapiro-Wilk, and Kolmogorov-Smirnov tests. Data were analyzed with two-tailed Mann–Whitney, unpaired Student t test, one-way analysis of variance (ANOVA), two-way ANOVA, or repeated-measures ANOVA, as applicable and Holm-Sidak's post hoc test for 2 by 2 comparisons. All tests were two tailed. Significance was considered $p < .05$. Detailed statistical results are reported in Table S3.

RESULTS

Striatal Regional Distribution and Regulation of *Ankk1* Messenger RNA

We first showed an enrichment of *Ankk1* messenger RNA (mRNA) expression in the DS as compared to the NAc (Figure 1A, A[i]). We next reanalyzed available RNA sequencing data from striatal extracts based on translating ribosome affinity purification technology (Figure 1B) (31) and showed that *Ankk1* mRNA is virtually absent in D1R-SPNs and selectively expressed in D2R-SPNs (Figure 1B[i]). We experimentally confirmed *Ankk1* mRNA enrichment in D2R-expressing neurons (Figure 1B) by performing real-time quantitative PCR on mRNA isolated by translating ribosome affinity purification selectively from D1R- and D2R-SPNs (Figure 1C). Next, we showed that stimulation of dopamine receptors by apomorphine treatment induced downregulation of *Ankk1* mRNA in both NAc and DS 1 and 3 hours after injection (Figure 1D, E).

We then assessed whether Ankk1 loss of function selectively in D2R-expressing neurons could recapitulate some of the phenotypes of A1 carriers. To do so, we generated Ankk1[lox/lox] mice in which exons 3–8 are flanked with LoxP sites allowing for Cre-targeted deletion of most of the Ankk1 gene (Figure 1F; Figure S1A), which we crossed with a Drd2-Cre line. Specificity of the recombination of the Ankk1 floxed locus was assessed by PCR on brain punches and peripheral tissues (Figure S1B). Cre-mediated decrease in *Ankk1* mRNA was also validated in the NAc of Ankk1[lox/lox]::Drd2-Cre^{+/-} (Ankk1[Δ-D2R N]) mice compared with control Ankk1[lox/lox]::Drd2-Cre^{-/-} (Ankk1[lox/lox]) mice (Figure 1G). However, because of the genetic construction of the Drd2-Cre bacterial artificial chromosome, which bears an additional copy of Ankk1 (32), crossing leads to a downregulation of Ankk1 rather than a full knock out in D2R-expressing neurons. Interestingly, we found a downregulation of ~24% of the *D2r* mRNA in Ankk1[Δ-D2R N] (Figure 1H), which resembles the ~30% reduction of striatal D2R availability in homozygous A1 allele carriers (23). Decreased D2R activity by downregulation of Ankk1 in D2R-expressing neurons was further supported by blunted cataleptic effects of haloperidol in Ankk1[Δ-D2R N] mice (Figure 1I) in both males and females (Figure S2A, B). These results suggest that the A1 variant in humans might be associated with a loss of function for the ANKK1 protein.

Specific Invalidation of Ankk1 in D2R Neurons Affects the Integrative Properties of D2R-SPNs

We next performed whole-cell patch clamp recording in brain slices of Ankk1[Δ-D2R N] and Drd2-Cre mice locally injected with a viral vector bearing a Cre-dependent mCherry reporter. First, we confirmed the downregulation of *Ankk1* mRNA in Ankk1[Δ-D2R N] as compared with Drd2-Cre mice (Figure 2A). D2R-SPNs were identified based on mCherry fluorescence (Figure 2B). Ankk1 downregulation did not affect basic membrane and synaptic properties in D2R-SPNs, as shown by resting membrane potential, resistance and rheobase (Figure 2C; Table S1), and amplitude and frequency of spontaneous excitatory (Figure 2D) and inhibitory (Figure 2E) postsynaptic currents. By contrast, paired-pulse response (50 ms interval) of excitatory inputs onto D2R-SPNs were reduced in Ankk1[Δ-D2R N] mice, compared with Drd2-Cre mice (Figure 2F), suggesting an enhanced presynaptic probability of glutamatergic inputs onto D2R-SPNs (33). Accordingly, spiking probability in response to electrical stimulation of excitatory afferents to the NAc was significantly enhanced in D2R-SPNs of Ankk1[Δ-D2R N] mice (Figure 2G), reflecting an increase in excitability (34). Overall, these data demonstrate that Ankk1 downregulation in D2R-expressing neurons enhances glutamatergic transmission onto D2R-SPNs, leading to increased excitability (35).

Effect of Ankk1 Downregulation in D2R-Expressing Neurons on Striatal-Related Learning

We next assessed the effect of Ankk1 downregulation on tasks known to strongly depend on striatal integrity. We first used striatal-dependent procedural learning, based on an egocentric strategy to learn to locate, without any external cues, the baited arm in a T-maze (36,37) (Figure 3A, right). Ankk1[Δ-D2R N] mice displayed a strong impairment in the ability to learn the location of the reward in the maze (Figure 3A), supporting a key role of Ankk1 in procedural learning. We next investigated performance of control and Ankk1[Δ-D2R N] mice in an operant conditioning paradigm (Figure 3B, right), another striatal-related associative task (38). Both male and female Ankk1[lox/lox] and Ankk1[Δ-D2R N] mice displayed similar discriminatory performances when analyzing the percentage of lever presses on the reinforced lever (Figures S2C–F and S3A, C, E, F). Ankk1[Δ-D2RN] displayed enhanced active lever pressing when operant ratios were increased (Figure 3B). Although this result suggests an enhanced motivational component in Ankk1[Δ-D2R N] mice, performances were similar to control mice in a progressive ratio task (Figure S3A–D). We also analyzed the time to initiate
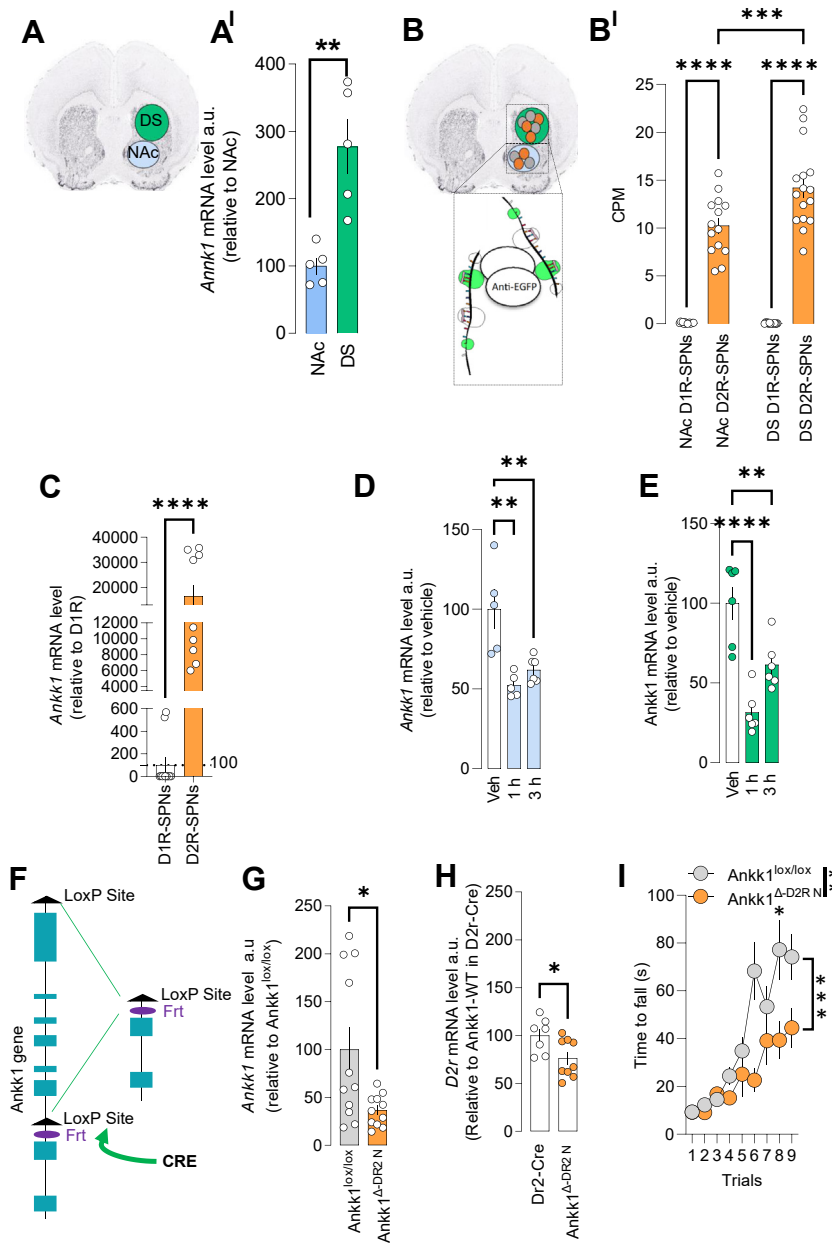
Figure 1. Ankk1 mRNA is expressed in the D2R-SPNs of the DS and NAc and its downregulation leads to a decrease of *D2r* mRNA. **(A)** Schematic representation of the dissected tissue samples on coronal sections of striatum. Brains were rapidly dissected and placed in a stainless-steel matrix with 0.5-mm coronal section interval. A thick slice containing the striatum (3 mm thick) was obtained. The DS (green) and the NAc (light blue) were punched out on ice. **(A^I)** mRNA was purified from the NAc and DS of C57BL/6 mice and analyzed by real-time quantitative polymerase chain reaction. The expression levels were calculated by the comparative delta-delta cycle threshold method with RPL19 as an internal control. Data points are individual results from different mice (*n* = 5 per group). Means ± SEM are indicated. Statistical analyses were performed using a two-tailed Mann-Whitney test, **p = .0079. **(B)** Schematic representation of the TRAP technique. Briefly, mRNA from either D2R- (orange) or D1R- (gray) SPNs were immunoprecipitated by using antibodies against the EGFP expressed in D2R or D1R ribosomes. **(B^I)** Analysis of available RNA sequencing data from TRAP reveals a specific enrichment of *Ankk1* mRNA in D2R-SPNs as compared with D1R-SPNs in both NAc and DS. Count per millions in each immunoprecipitation are reported. Data points are individual results from different pools of mice. Means ± SEM are indicated. Statistical analyses were performed using two-way ANOVA: interaction $F_{1,56}$ = 8.643, *p* = .0048, Nucleus Accumbens/Dorsal Striatum NAc/DS $F_{1,32}$ = 8.25, *p* = .0057, D1/D2 SPNs: $F_{1,56}$ = 319.5, *p* < .0001 Tukey's post hoc test ****p < .0001, ***p = .0007. **(C)** mRNA level of Ankk1 in isolated D1R- or D2R-SPN populations, analyzed by real-time quantitative polymerase chain reaction from male and female transgenic D1- and D2-TRAP mice. Statistical analyses were performed using two-tailed Mann-Whitney unpaired *t* test: ****p < .0001. **(D, E)** mRNA level of *Ankk1* in the NAc **(D)** and the DS **(E)** of mice injected with either saline or apomorphine (3 mg/kg) and sacrificed 1 and 3 hours after injections. Data points are individual results from different mice (*n* = 5–6 per group). Means ± SEM are indicated. **(D)** Statistical analyses NAc: one-way ANOVA: *F* = 11.47 *p* = .0013 followed by Dunnett's multiple comparison *p* = .0012, and *p* = .0045. **p < .01. **(E)** DS, one-way ANOVA, *F* = 20.87 *p* < .0001 followed by Dunnett's multiple comparison ****p < .0001, **p = .0046. **(F)** Strategy of production of *Ankk1* floxed mice. **(G)** *Ankk1* mRNA levels from the NAc of Ankk1$^{lox/lox}$ and Ankk1$^{\Delta-D2R\ N}$ mice. Data are reported as means ± SEM of results of individual mice (*n* = 11); statistical analyses were performed with two-tailed Mann-Whitney unpaired *t*

test: *p = .0473. **(H)** *D2r* mRNA level from the NAc of Drd2-Cre and Ankk1$^{\Delta-D2R\ N}$ mice. Data are reported as means ± SEM of results of individual mice (*n* = 7–9). Statistical analyses were performed with nonparametric Mann-Whitney test, *D2r* *p = .0418. **(I)** The effects of *Ankk1* and *D2r* mRNA downregulation on D2R function were investigated by evaluating catalepsy after haloperidol injection (0.1 mg/kg intraperitoneal). Statistical analyses were performed using two-way ANOVA (18 mice per group): interaction *p* = .0008, genotype *p* = .0020, followed by Sidak's post hoc test: line 6 *p* = .018. ***p < .001, **p < .01, *p < .05. ANOVA, analysis of variance; CPM, counts per million; D2R, D$_2$ receptor; DS, dorsal striatum; EGFP, enhanced green fluorescent protein; mRNA, messenger RNA; NAc, nucleus accumbens; SPN, spiny projection neuron; TRAP, translating ribosome affinity purification.

and complete the operant task and found no significant difference between control and Ankk1$^{\Delta-D2R\ N}$ mice. Our findings show that downregulation of Ankk1 in D2R-expressing neurons leads to deficits in an egocentric strategy-based procedural learning task as well as in reward-driven operant conditioning paradigms.

Ankk1 Loss of Function in D2R-Expressing Neurons Does Not Alter Energy Homeostasis on a Regular Chow Diet

Given the emerging link between reward-dependent behavior and energy homeostasis metabolism ([39](#)), we next explored the consequence of Ankk1 knockdown on metabolic efficiency
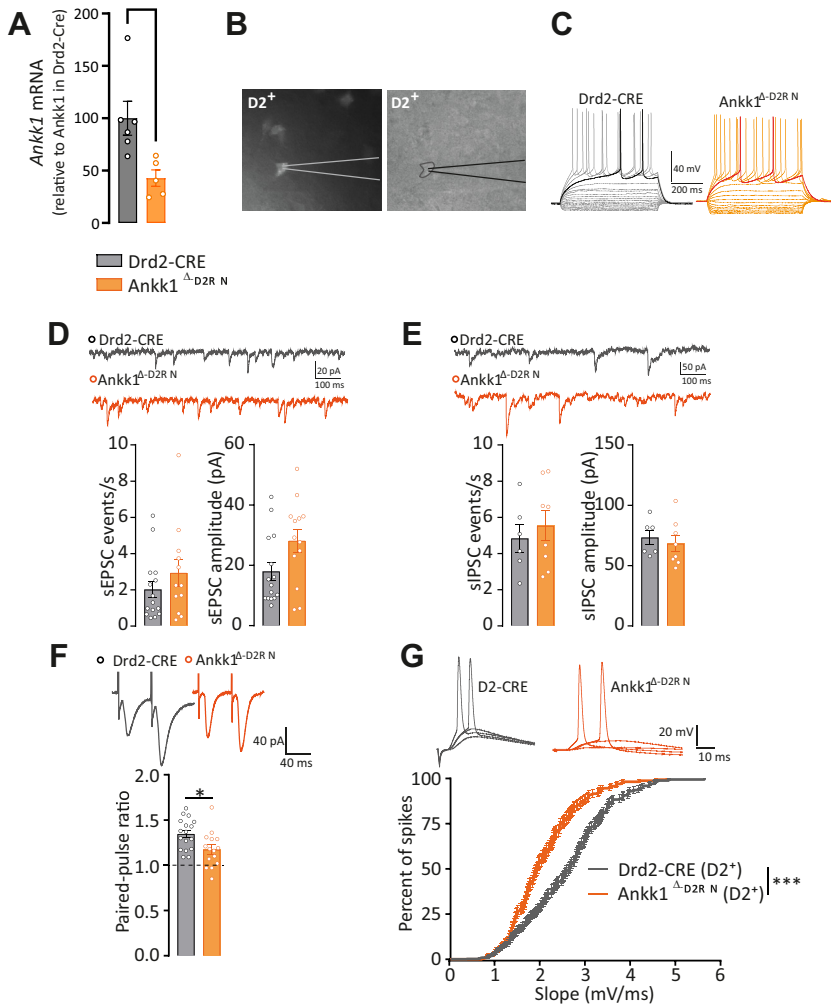
Figure 2. Ankk1 downregulation in D2R-expressing neurons increases their excitability. **(A)** mRNA level of *Ankk1* in the NAc of Drd2-Cre and Ankk1$^{\Delta\text{-D2R N}}$ mice. **(B)** Male and female Drd2-Cre and Ankk1$^{\Delta\text{-D2R N}}$ mice were stereotaxically injected with a viral vector carrying a flex AAV-mCherry. D2R-SPNs in the NAc were identified based on red fluorescence and patched. **(C)** Illustrative voltage responses of D2R-SPNs recorded in Drd2-Cre (gray, left) and Ankk1$^{\Delta\text{-D2R N}}$ (orange, right) mice in response to a series of 600-ms current pulses starting at −150 pA with 20 pA increments. **(D)** Ankk1 downregulation does not alter frequency (left) or amplitude (right) of sEPSCs. Mann-Whitney unpaired *t* test *p* = .39 and *p* = .09, respectively (Drd2-Cre: *n* = 15 neurons in 9 mice; Ankk1$^{\Delta\text{-D2R N}}$: *n* = 14 neurons in 9 mice). **(E)** Ankk1 downregulation does not alter frequency (left) or amplitude (right) of sIPSCs. Mann-Whitney unpaired *t* test *p* = .59 (Drd2-Cre: *n* = 6 neurons in 3 mice, Ankk1$^{\Delta\text{-D2R N}}$: *n* = 8 neurons in 3 mice). **(F)** In PPR experiments, excitatory fibers were stimulated twice with an interval of 50 ms, while EPSCs were monitored in voltage clamp. In D2R-SPNs, Ankk1 downregulation resulted in a decrease of PPR. Two-tailed Mann-Whitney unpaired *t* test, **p* = .0171 (Drd2-Cre: *n* = 17 neurons in 10 mice; Ankk1$^{\Delta\text{-D2R N}}$: *n* = 15 neurons in 9 mice). **(G)** The excitability of D2R-SPNs in the NAc was measured by quantifying the spiking probability with increasing electrical stimulation of excitatory inputs. The spiking probability is represented as a function of EPSP slope (mV/ms). Excitability of D2R-SPNs is increased in Ankk1$^{\Delta\text{-D2R N}}$ mice (****p* < .0001) (Drd2-Cre: *n* = 18 neurons in 12 mice; Ankk1$^{\Delta\text{-D2R N}}$: *n* = 10 neurons in 8 mice). AAV, adeno-associated virus; D2R, D₂ receptor; DS, dorsal striatum; EGFP, enhanced green fluorescent protein; EPSP, excitatory postsynaptic potential; mRNA, messenger RNA; NAc, nucleus accumbens; PPR, paired pulse ratio; sEPSC, spontaneous excitatory postsynaptic current; sIPSC, spontaneous inhibitory postsynaptic current; SPN, spiny projection neuron.

in mice fed ad libitum with a standard diet. Food intake, locomotor activity, metabolic efficiency, and selective carbohydrates versus lipid substrate utilization in Ankk1$^{lox/lox}$ and Ankk1$^{\Delta\text{-D2R N}}$ mice were measured as previously described

(30). Both Ankk1$^{lox/lox}$ and Ankk1$^{\Delta\text{-D2R N}}$ mice were comparable for body weight (Figure S4A), body composition (Figure S4B, C, D), locomotor activity (Figure S4E), energy intake (Figure S4F), energy expenditure (Figure S4G), and whole-body
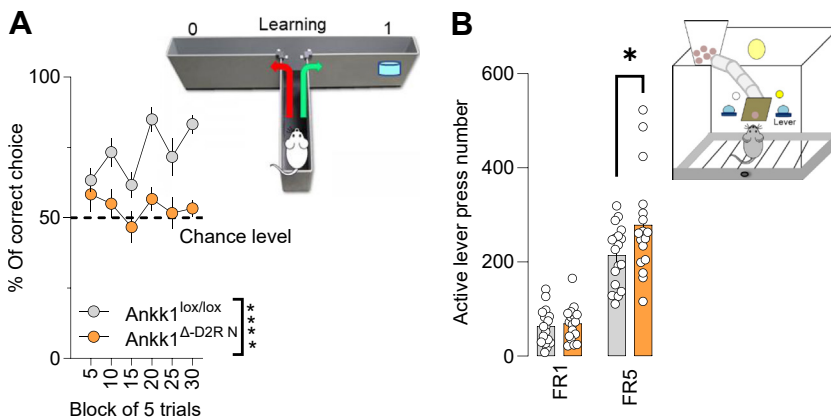

Figure 3. Consequences of Ankk1 downregulation in D2R-expressing neurons on striatal-dependent behaviors and energy metabolism. **(A)** Effect of downregulation of Ankk1 on procedural learning. Acquisition of the food-rewarded arm choice in a T-maze is impaired in Ankk1$^{\Delta\text{-D2R N}}$ mice. Statistical analyses were performed with two-way ANOVA: interaction *p* = .12, genotype *****p* < .0001, *n* = 12 (males 6–8, females 6–4). **(B)** Average of active lever press across FR1 and FR5 of instrumental conditioning, statistical analyses were performed with two-way ANOVA: interaction *p* = .0115, genotype *p* = .0964, time (learning) *p* < .0001, followed by Sidak's multiple comparison **p* = .014, *n* = 18 (males 12–13, females 6–4). ANOVA, analysis of variance; D2R, D₂ receptor; FR, fixed ratio.

fatty acid oxidation (Figure S4H). Two-way ANOVA of food intake showed a significant interaction in genotype per time, with no significant genotype differences (Figure S4H). Similar results were obtained when male and female mice were analyzed separately (Figure S5A–P).

D2R-Neuron–Specific Ankk1 Knockdown Leads to Changes in Nutrient Partitioning and Protection From Diet-Induced Obesity

Various studies have associated variations of Ankk1 with metabolic changes and, more specifically, with obesity (40–42). Hence, we next explored whether the interaction

between genotype and obesogenic environment would unveil alterations in energy homeostasis regulation in Ankk1$^{\Delta\text{-D2R N}}$. Therefore, we subjected Ankk1$^{\text{lox/lox}}$ and Ankk1$^{\Delta\text{-D2R N}}$ mice to 3 months of a high-fat high-sucrose diet (HFHS) prior to metabolic characterization. Obese mice (Ob-Ankk1$^{\Delta\text{-D2R N}}$ and Ob-Ankk1$^{\text{lox/lox}}$) showed comparable body weight (Figure 4A) and lean mass (Figure 4B), however, fat mass was decreased in Ob-Ankk1$^{\Delta\text{-D2R N}}$ mice (Figure 4C, D). Ob-Ankk1$^{\Delta\text{-D2R N}}$ and control mice also displayed similar locomotor activity (Figure 4E), caloric intake (Figure 4F), and a trend toward decreased energy expenditure (p = .12) (Figure 4G). Interestingly, upon consumption of the obesogenic diet, Ankk1$^{\Delta\text{-D2RN}}$
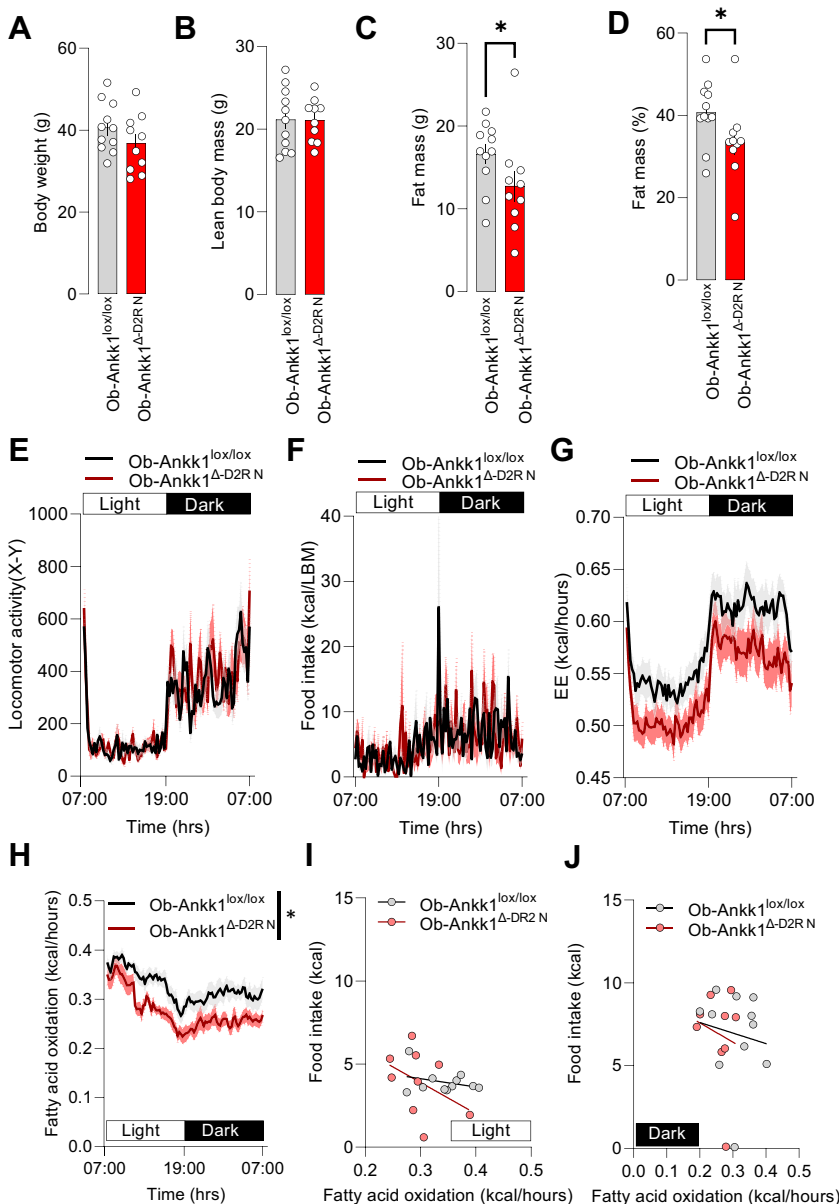
Figure 4. Consequences on metabolism of Ankk1 downregulation in D2R-expressing neurons in a diet-induced obesity paradigm. Ankk1$^{\Delta\text{-D2R N}}$ mice do not show alteration in body weight **(A)** and lean mass **(B)**; however, they do show significant decreases in fat mass p = .037 **(C)** and fat mass % p = .0430 **(D)** (two-tailed Mann-Whitney n = 11–10, males 5–6, females 6–4). Ankk1$^{\Delta\text{-D2R N}}$ and control mice show similar locomotor activity **(E)**, food intake **(F)**, and energy expenditure **(G)**. Ankk1$^{\Delta\text{-D2R N}}$ mice showed decreased fatty acid oxidation **(H)**, two-way ANOVA: interaction p = .4487, genotype p = .0221, time p < .0001. Fatty acid oxidation does not correlate with kcal intake in either light **(I)** or dark **(J)** phase. *p < .05. ANOVA, analysis of variance; D2R, D$_2$ receptor; EE, energy expenditure.

displayed a decreased level in fatty acid oxidation (Figure 4H). Such a decrease does not seem to depend on the kilocalorie intake, as shown by the lack of correlation between food intake and fatty acid oxidation (Figure 4I, J). This finding reveals that an obesogenic downregulation of Ankk1 in D2R-expressing neurons is sufficient to induce alterations in peripheral substrate utilization and nutrient partitioning (43,44).

Region-Specific Invalidation of Ankk1 in the Ventral or Dorsal Part of the Striatum Differentially Affect Reward-Driven Behavior

To unveil the neuroanatomical specificity of Ankk1 loss of function within the striatum, we compared the consequence of viral-mediated knockdown of Ankk1 in the DS or NAc. Littermate Ankk1$^{lox/lox}$ mice received stereotactic injection of AAV-GFP or AAV-Cre in the NAc or in DS to produce controls (Ankk1$^{GFP-NAc}$ and Ankk1^{GFP-DS}) or Ankk1 knockdown (Ankk1$^{\Delta-NAc}$ and Ankk1$^{\Delta-DS}$). Accuracy of injection site and consequent change in *Ankk1* levels were assessed through viral-mediated expression of GFP and real-time quantitative PCR (Figure S6A, B for the DS and Figure S6E, F for the NAc). Downregulation of Ankk1 in the DS did not affect the levels of *D2r* mRNA (Figure S6C) or haloperidol-induced catalepsy (Figure S6D); however, knockdown of Ankk1 in the NAc significantly decreased *D2r* mRNA levels (Figure S6G) and blunted haloperidol-induced cataleptic events similar to Ankk1$^{\Delta-D2RN}$ mice (Figure S6H). Furthermore, as for Ankk1$^{\Delta-D2RN}$, Ankk1$^{\Delta-NAc}$ mice displayed an impairment in learning the egocentric strategy in the T-maze task (Figure 5A), together with enhanced lever pressing from lower ratio requirement in the operant conditioning paradigm (Figure 5B). In this latter task, Ankk1$^{\Delta-NAc}$ mice exerted significantly more lever presses on the nonreinforced lever, while performance in the progressive ratio task was unchanged (Figure S7A, B). Ankk1$^{\Delta-NAc}$ mice also produced significantly more lever presses on the active lever during the inactive phase, a proxy for impulsive behavior (45). These behavioral alterations were observed in both ad libitum and fasting, indicating that this phenotype is not strictly dependent on hunger state (Figure S7C, D). We also analyzed the time to initiate and complete the operant task and found no significant difference between control and Ankk1$^{\Delta-NAc}$ mice.

Altogether, our findings demonstrate that Ankk1 loss of function in the NAc is sufficient to recapitulate some of the behavioral phenotypes of Ankk1$^{\Delta-D2R\ N}$ mice. By contrast, Ankk1$^{\Delta-DS}$ mice had similar performance to control mice in both the learning phase of the T-maze paradigm and in operant conditioning for both ratio requirements. However, Ankk1$^{\Delta-DS}$ mice displayed a selective deficit in the reversal phase of the T-maze (Figure S8A, B). This latter finding resembles impaired cognitive flexibility described in Taq1A carriers (15,46).

Striatal Deletion of Ankk1 Alters Energy Homeostasis

We next assessed metabolic parameters in Ankk1$^{\Delta-DS}$ and Ankk1$^{\Delta-NAc}$ mice. Ankk1 loss of function in the NAc did not result in any significant changes in body weight (Figure 5C) or lean mass (Figure 5D) but decreased fat mass (Figure 5E) and fat mass % (Figure 5F). As for the Ankk1$^{\Delta-D2R\ N}$ groups, Ankk1$^{\Delta-NAc}$ mice showed unaltered locomotor activity

(Figure 5G) and caloric intake (Figure 5H), although a trend was detected (genotype $p = .056$, interaction $p = .06$). Moreover, Ankk1$^{\Delta-NAc}$ displayed a decrease in energy expenditure (Figure 5I) and fatty acid oxidation (Figure 5J), indicating that loss of function of Ankk1 specifically influences peripheral nutrient utilization. Change in fatty acid oxidation correlated with caloric intake (Figure 5K, L) but was independent from body weight and lean mass, which were comparable between the two genotypes (Figure 5C, D). Interestingly, fatty acid oxidation mostly decreased during the light phase (Figure 5L), which might indicate a dissociation between circadian-entrained rhythm and whole-body fatty acid oxidation (47,48). Importantly, when tested on a binge eating paradigm with HFHS, a test aimed at evaluating uncontrolled voracious eating, Ankk1$^{\Delta-NAc}$ mice showed enhanced food consumption during the binge period (Figure S5E). We next explored whether the obesogenic environment could magnify the metabolic consequence of Ankk1 knockdown. Mice were fed HFHS for 3 months prior to the replication of the metabolic efficiency assessment. As compared with obese controls (Ob-Ankk1$^{GFP-NAc}$), Ob-Ankk1$^{\Delta-NAc}$ mice showed a decrease in body weight (Figure 6A), comparable lean mass (Figure 6B), a decrease in fat mass (Figure 6C), and a tendency toward decreasing fat mass % (Figure 6D). Ob-Ankk1$^{\Delta-NAc}$ mice showed comparable caloric intake (Figure 6E) but higher locomotor activity (Figure 6F) and decreased energy expenditure (Figure 6G). As for Ob-Ankk1$^{\Delta-D2RN}$, Ob-Ankk1$^{\Delta-NAc}$ mice displayed lower fatty acid oxidation (Figure 6H), which was independent from food intake (Figure 6I, J). Overall, these data indicate that Ankk1 loss of function in the NAc exerts some protective effect from HFHS-induced disturbance in nutrient intake and partitioning. On the contrary, Ankk1 loss of function in the DS did not result in any relevant alteration in body weight and composition (Figure S6D, G), locomotor activity (Figure S6H), feeding (Figure S6I), or energy expenditure (Figure S6J). However, we could observe a small difference in the light-dark phase distribution of whole fatty acid oxidation in Ankk1$^{\Delta-DS}$ mice (Figure S6H). No difference between groups was observed in the binge eating paradigm (Figure S6C). These results underscore the neuroanatomical discrimination of Ankk1-dependent regulation of metabolism in the striatum.

Differential Respiratory Quotient as a Function of Taq1A A1 Allele Status in Human Participants

Given the change in nutrient partitioning associated with Ankk1 loss of function in mice, we hypothesized that a qualitatively similar phenotype could arise from the A1/A2 variant in humans. We used indirect calorimetry during resting state to calculate the RQ, the ratio between carbon dioxide (CO_2) and oxygen (O_2), indicative of substrate utilization (RQ = 1 for carbohydrate and RQ = 0.7 for lipid) in 32 healthy human participants (19 A1− and 13 A1+) (Figure 7). Age, fat mass, and other anthropometric measures were similar for both genotypes (Table S2). The groups also did not differ in hours of sleep and hours since last meal prior to the metabolic measure (Table S2). However, there was a significant difference in sex distribution between A1+ and A1− groups ($p = .0014$) (Table S2), so this factor was included in statistical models. Consistent with the observations in mice, A1+ individuals
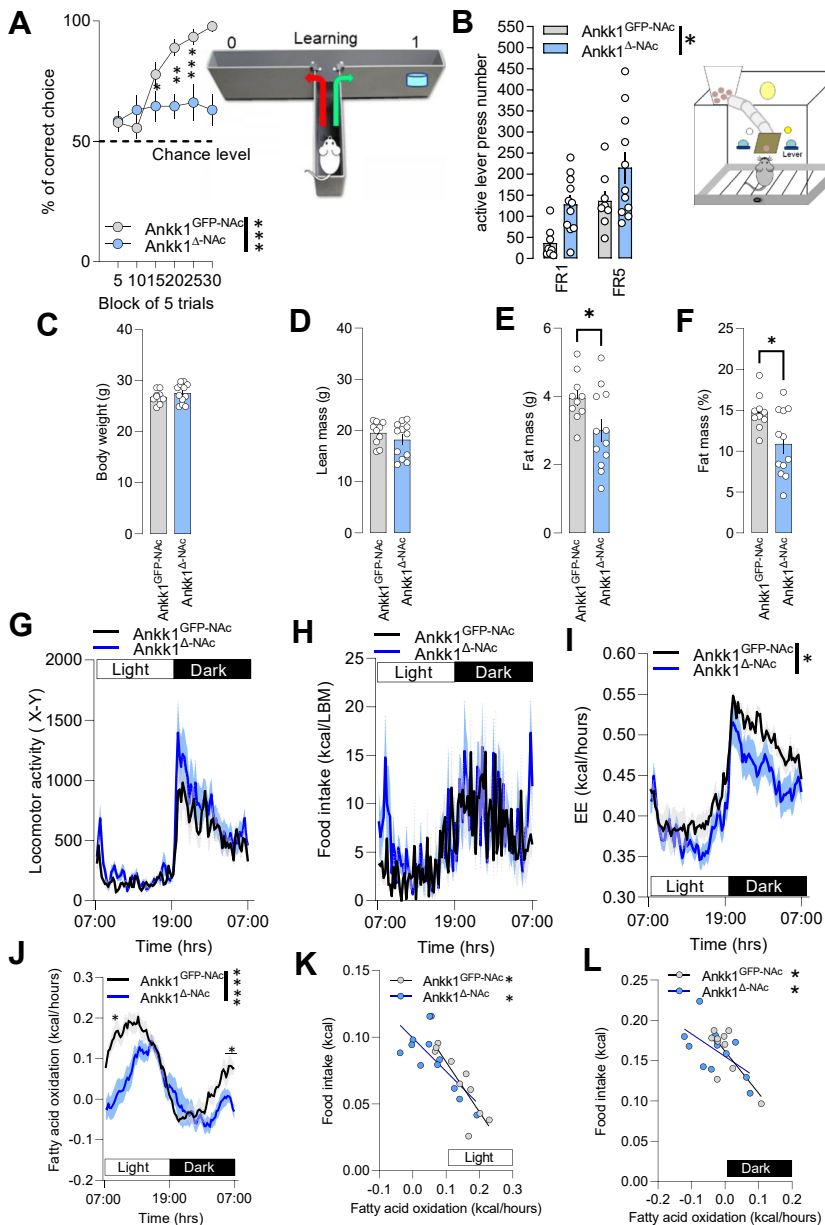
Figure 5. Consequences of Ankk1 downregulation in the NAc on striatal-dependent behaviors and energy metabolism. **(A)** Effect of Ankk1 loss of function in the NAc on procedural learning. Acquisition of the food-rewarded arm choice in a T-maze is impaired in Ankk1$^{\Delta\text{-NAc}}$ mice. Statistical analyses were performed with two-way ANOVA: interaction ***p = .0004, time p < .0001, genotype p < .0001. Sidak's multiple comparison *p = 0.0176, **p = 0.0055, ***p = 0.0002; n = 9–13 (males 5–8, females 4–5). **(B)** Average of active lever press across FR1 and FR5 of instrumental conditioning is increased in Ankk1$^{\Delta\text{-NAc}}$ as compared with Ankk1$^{\text{GFP-NAc}}$. Statistical analyses were performed using two-way ANOVA: interaction p = .776, learning p = .0006, genotype p = .0162. n = 8–11 (males 4–6, females 4–5). **(C)** Ankk1 loss of function in the NAc does not alter body weight **(C)** and lean mass **(D)** but decreases fat mass **(E)** and fat mass % **(F)**; statistical analyses were performed with two-tailed t test: t_{20} = 2.284, p = .0335; fat mass t_{20} = 2.696, p = .0139, respectively. Data are expressed as mean ± SEM. n = 10–13 (males 5–7, females 5-5). Ankk1$^{\Delta\text{-NAc}}$ and Ankk1$^{\text{GFP-NAc}}$ showed comparable locomotor activity **(G)** and food intake **(H)**; however, Ankk1$^{\Delta\text{-NAc}}$ display decreased energy expenditure **(I)**, statistical analysis by two-way ANOVA: interaction *p = .034, time p < .0001, p = .108, and fatty acid oxidation **(J)**; statistical analysis by two-way ANOVA: interaction ****p < .0001, time p < .0001, genotype p = .0075 Sidak's post hoc test *p < .05. Fatty acid oxidation significantly correlates with food intake for both light **(K)** and dark **(L)** phases. Statistical analysis light phase: Ankk1$^{\text{GFP-NAc}}$ *p = .0009, Ankk1$^{\Delta\text{-NAc}}$ *p = .0083. Statistical analysis dark phase: Ankk1$^{\text{GFP-NAc}}$ *p = .0152, Ankk1$^{\Delta\text{-NAc}}$ *p = .0441. ****p < .0001. ANOVA, analysis of variance; EE, energy expenditure; FR, fixed ratio; NAc, nucleus accumbens.

showed a significantly higher resting RQ compared with A1− individuals (R^2 = 0.41, F_6 = 7.31, p = .012). This result suggests a shift toward carbohydrate use as a primary energy source in A1+ and a shift toward fat in A1− at rest. This indicates that the polymorphism affecting the *ANKK1* gene in humans does alter peripheral nutrient utilization. These data support our reverse translational approach and show that the metabolic phenotype observed in mice translates to humans.

DISCUSSION

In this study, we showed for the first time that *Ankk1* mRNA is enriched in striatal D2R-SPNs and that its downregulation in D2R-expressing neurons is sufficient to alter their activity and to decrease *D2r* mRNA expression and D2R-mediated response. These changes were associated with altered performance in striatal-dependent tasks such as procedural learning and reward-driven operant conditioning. Both D2R-specific and accumbal-restricted knockdown of Ankk1 were similarly associated with change in nutrient partitioning, suggesting a role for Ankk1 in striatal control of energy homeostasis. Finally, we performed a translational study that, in accordance with the mouse data, revealed differential whole-body metabolism in A1 carriers versus noncarriers.

The reduction of *D2r* mRNA expression transcript as a consequence of Ankk1 knockdown are congruent with
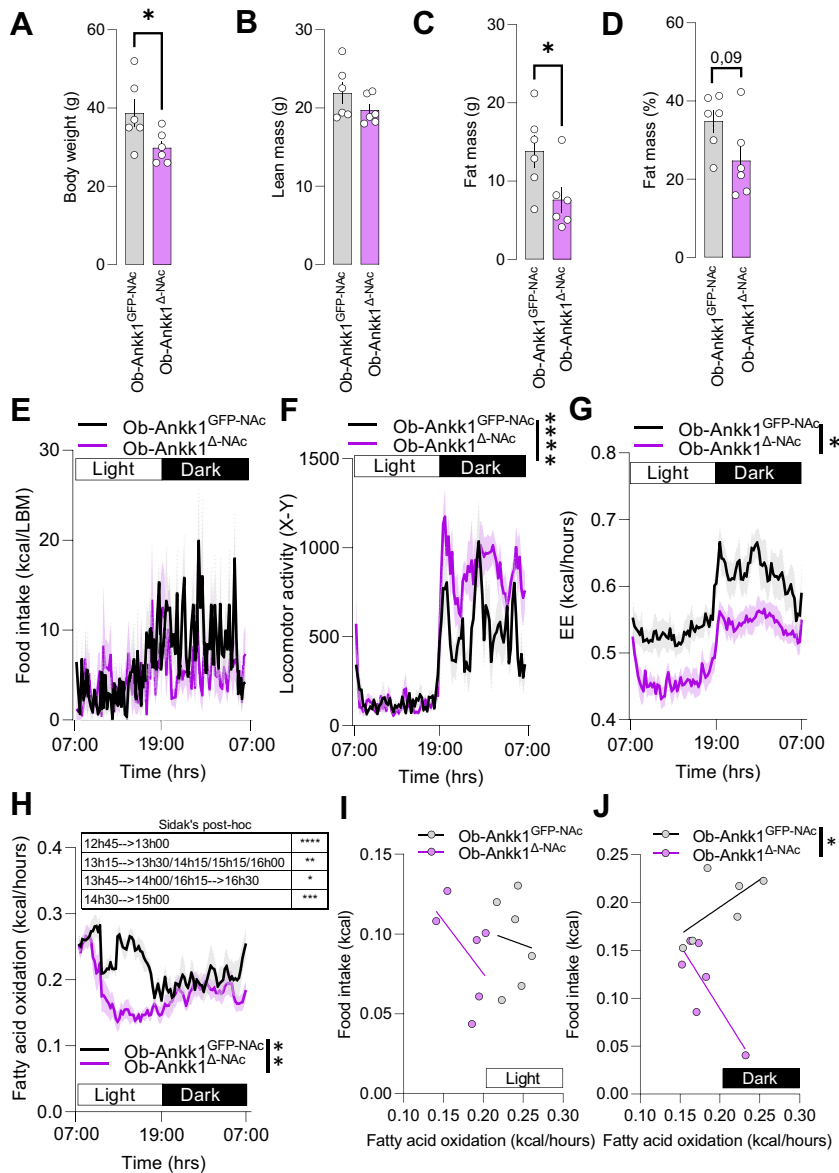
Figure 6. Consequences of Ankk1 loss of function in the NAc on metabolism in a diet-induced obesity paradigm. Ankk1$^{\Delta\text{-NAc}}$ display decreased body weight **(A)** two-tailed Mann-Whitney test, $p = .0455$, but not lean mass **(B)**, and decreased fat mass **(C)** two-tailed Mann-Whitney test, $p = .0411$, but not fat-mass percentage **(D)** two-tailed Mann-Whitney test, $p = .0931$. **(E)** Caloric intake is comparable between Ankk1$^{\text{GFP-NAc}}$ and Ankk1$^{\Delta\text{-NAc}}$, but the Ankk1$^{\Delta\text{-NAc}}$ group showed increased locomotor activity **(F)** and decreased energy expenditure **(G)**. Statistical analyses in **(F)** were performed using two-way ANOVA: interaction $p < .0001$, time $p < .0001$, genotype $p = .0138$. Statistical analyses in **(G)** were performed using two-way ANOVA: interaction $p < .0001$, time $p < .0001$, genotype $p = .0222$. **(H)** Downregulation of Ankk1 in the NAc decreases fatty acid oxidation; statistical analyses were performed with two-way ANOVA: interaction $p < .0001$, time $p < .0001$, genotype $p = .0074$. Sidak's post hoc test, $*p < .05$, $**p < .001$, $***p < .0001$. **(I, J)** Fatty acid oxidation does not significantly correlate with food intake in both light **(I)** and dark **(J)** phases; however, in the dark phase, slopes of the regression lines are significantly different between the 2 groups, $p = .0129$ **(J)**. Data are expressed as mean ± SEM, $n = 6$ (male 2–4, female 2–4). $****p < .0001$. ANOVA, analysis of variance; EE, energy expenditure; NAc, nucleus accumbens.

published studies pointing at the consequences of TaqIA variants on D2R abundance, D2R-dependent function (23–25), and impaired reward-related behaviors (49,50). The increase in D2R-SPN activity is consistent with impaired reward-related behaviors (49,51), in particular, regarding the NAc.

In fact, viral-mediated deletion of Ankk1 selectively in the NAc during adulthood recapitulates and even amplifies some of the behavioral phenotypes obtained in Ankk1$^{\Delta\text{-D2R N}}$, such as alteration in procedural learning and operant behavior. The consistent deficits we observed in the T-maze task for both Ankk1$^{\Delta\text{-D2R N}}$ and Ankk1$^{\Delta\text{-NAc}}$ are unlikely to be solely related to learning inabilities. In fact, even though it has been shown that the T-maze task relies on propriocentric and egocentric strategies that depend on the integrity of the striatum (52), manipulations of the NAc can spare the acquisition of action-

outcome associations, while impairing flexible adaptation of previously learned rules (53,54) in particular when interfering with D2R-SPNs (55). In accordance, both Ankk1$^{\Delta\text{-D2R N}}$ and Ankk1$^{\Delta\text{-NAc}}$ were capable of learning the association between lever pressing and reward obtainment. However, Ankk1$^{\Delta\text{-NAc}}$ also displayed an increased number of lever presses on the nonrewarded lever, as well as enhanced active lever pressing during the timeout period, a feature considered as a proxy for impulsivity (45,56).

This suggests that the increased operant conditioning responding in Ankk1$^{\Delta\text{-NAc}}$ as well as Ankk1$^{\Delta\text{-D2R N}}$ mice might result from increased impulsivity. Importantly, impulsivity has been associated with decreased D2R availability in the NAc (45,57) and represents a main feature of A1 carriers (21,22,58,59). Additionally, selective impairment in the reversal
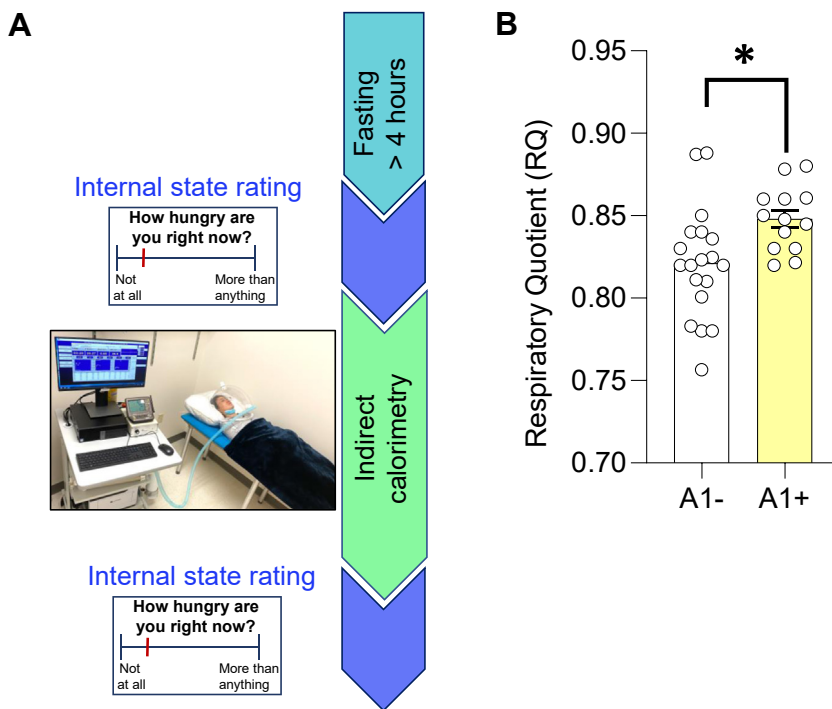
A

Internal state rating

How hungry are you right now?

Not at all — More than anything

Internal state rating

How hungry are you right now?

Not at all — More than anything

Fasting > 4 hours

Indirect calorimetry

B

Figure 7. Resting RQ between A1 allele carriers (A1+) and non-A1 carriers (A1−) of Taq1A polymorphism (rs1800497). **(A)** Protocol design. Thirty-two participants with healthy weight (body mass index < 26) underwent metabolic measurements using indirect calorimetry and genotyping from saliva. **(B)** Respiratory quotient measures, data points are individual results from different participants (*n* = 19 in A1− and *n* = 13 in A1+). Means + SEM are indicated. Statistical analysis was performed with an independent *t* test and controlled for body mass index, sex, age, and study. *p = .012. RQ, respiratory quotient.

phase of the T-maze in Ankk1$^{\Delta-DS}$ mice resembles decreased cognitive flexibility observed in TaqIA individuals (15,46). Altogether, the behavioral effects obtained under Ankk1 loss of function are in line with poorer negative outcome learning (60,61) and procedural learning (62), increased impulsivity (21,22,58,59), altered prediction error (60), weaker reward sensitivity [for a review, see (63)], and impaired cognitive flexibility (15,46) associated with the A1 allele.

Of note, in addition to D2R-SPNs, cholinergic interneurons also express *D2r* and therefore could be affected by Drd2-Cre–mediated Ankk1 knockdown. While the presence of Ankk1 in cholinergic interneurons remains elusive, one cannot rule out that loss of Ankk1 in cholinergic interneurons using a Drd2-Cre driver could contribute to the behavioral and metabolic outputs we observed, given the prominent role of cholinergic interneurons in various striatal functions (31,64).

In addition to the behavioral consequences of Ankk1 knockdown on reward-related behaviors, the present study demonstrates a role for Ankk1 integrity in the control of peripheral substrate utilization in both rodents and humans. In both rodent models of Ankk1 knockdown, the metabolic changes were magnified. This is particularly relevant in the context of interactions of genetic polymorphisms, including Taq1A, and the modern food environment [for review, see (63)] as a risk factor for pathological conditions. Furthermore, while vulnerability for the metabolic defect in Taq1A carriers has been largely attributed to altered reward feeding and over-consumption, the link we established between Ankk1 integrity and nutrient partitioning suggests that an additional component of central control of energy homeostasis might be at play, independent from caloric intake. This is in line with the

associations with TaqIA and insulin sensitivity (41) and as a modulator of weight loss induced by monoamine reuptake inhibitor treatment (40).

In our mice models, Ankk1 loss of function paradoxically seems to protect against increases in body weight and fat mass. This could be the result of an overall change in inter-organ communication and metabolic fluxes (43). Yet, the A1 polymorphism has also been associated with accelerated weight loss (40) and some features of anorexia (13), which share common symptomatic dimensions with compulsive eating, such as deficit in cognitive flexibility, impaired reward processing, and impulsivity (65). However, while the decreased *D2r* mRNA levels under Ankk1 loss of function together with diminished adiposity seem counterintuitive because a decrease in D2r in the DS has been associated with obesity (27), the developmental increase in *D2r* has been linked to enhanced predisposition for obesity and metabolic defects (64), and various studies suggest the decrease in D2R levels could correlate with other dimensions linked to obesity that are independent from BMI, such as opportunistic eating or decreased locomotor activity (28). Moreover, although fewer studies are available regarding the NAc, findings in humans and rodents reveal a negative association between ventral striatal D2R and BMI (66), increased D2R in the ventral striatum of obese subjects, and increased accumbal D2R levels following exposure to fat diets (67).

Several molecular mechanisms could account for the decrease in *D2r* and defective D2R-neurons in our model of Ankk1 loss of function or in the TaqIA carrier. Ankk1 has been found to exert transcriptional control of the nuclear factor-kappa B (NF-κB)–regulated gene (68). Because

2 NF-κB–responsive elements exist in the *D2r* promoter and positively regulate *D2r* transcription (69), it is possible that a reduced dosage of Ankk1 in heterozygous human carriers and in our animal model of loss of function could lead to decreased D2r abundance and altered D2R-SPN functions (23,24).

In conclusion, this work provides the first reverse translational approach exploring the biological functions of Ankk1 in the central regulation of both metabolic and reward functions and further translates the metabolic phenotype discovered in mice to humans. Collectively, our data show that Ankk1 loss of function is sufficient to mimic some of the phenotypic characteristics of Taq1A individuals and point toward Ankk1 as a potential molecular hub connecting striatal D2R-SPNs to the control of energy homeostasis.

A limitation of our study is the lack of precise molecular mechanisms. We cannot rule out the possibility that D_2 receptor abundance is the sole mechanism by which ANKK1 alters D2R-neuron physiology. Future studies are warranted to explore whether and how ANKK1 could be targeted for the treatment of psychiatric and metabolic diseases.

ACKNOWLEDGMENTS AND DISCLOSURES

REFERENCES

1. Insel T, Cuthbert B, Garvey M, Heinssen R, Pine DS, Quinn K, *et al.* (2010): Research domain criteria (RDoC): Toward a new classification framework for research on mental disorders. Am J Psychiatry 167:748–751.
2. Mitchell AJ, Vancampfort D, Sweers K, van Winkel R, Yu W, De Hert M (2013): Prevalence of metabolic syndrome and metabolic abnormalities in schizophrenia and related disorders—A systematic review and meta-analysis. Schizophr Bull 39:306–318.
3. Geschwind DH, Flint J (2015): Genetics and genomics of psychiatric disease. Science 349:1489–1494.
4. Neville MJ, Johnstone EC, Walton RT (2004): Identification and characterization of ANKK1: A novel kinase gene closely linked to DRD2 on chromosome band 11q23.1. Hum Mutat 23:540–545.
5. Mota NR, Araujo-Jnr EV, Paixão-Côrtes VR, Bortolini MC, Bau CH (2012): Linking dopamine neurotransmission and neurogenesis: The evolutionary history of the NTAD (NCAM1-TTC12-ANKK1-DRD2) gene cluster. Genet Mol Biol 35:912–918.
6. Pan YQ, Qiao L, Xue XD, Fu JH (2015): Association between ANKK1 (rs1800497) polymorphism of DRD2 gene and attention deficit hyperactivity disorder: A meta-analysis. Neurosci Lett 590:101–105.
7. McGuire V, Van Den Eeden SK, Tanner CM, Kamel F, Umbach DM, Marder K, *et al.* (2011): Association of DRD2 and DRD3 polymorphisms with Parkinson's disease in a multiethnic consortium. J Neurol Sci 307:22–29.
8. Meyers JL, Nyman E, Loukola A, Rose RJ, Kaprio J, Dick DM (2013): The association between DRD2/ANKK1 and genetically informed measures of alcohol use and problems. Addict Biol 18:523–536.
9. Voisey J, Swagell CD, Hughes IP, van Daal A, Noble EP, Lawford BR, *et al.* (2012): A DRD2 and ANKK1 haplotype is associated with nicotine dependence. Psychiatry Res 196:285–289.
10. Tsou CC, Chou HW, Ho PS, Kuo SC, Chen CY, Huang CC, *et al.* (2019): DRD2 and ANKK1 genes associate with late-onset heroin dependence in men. World J Biol Psychiatry 20:605–615.
11. Comings DE, Flanagan SD, Dietz G, Muhleman D, Knell E, Gysin R (1993): The dopamine D2 receptor (DRD2) as a major gene in obesity and height. Biochem Med Metab Biol 50:176–185.
12. Noble EP, Noble RE, Ritchie T, Syndulko K, Bohlman MC, Noble LA, *et al.* (1994): D2 dopamine receptor gene and obesity. Int J Eat Disord 15:205–217.
13. Nisoli E, Brunani A, Borgomainerio E, Tonello C, Dioni L, Briscini L, *et al.* (2007): D2 dopamine receptor (DRD2) gene Taq1A polymorphism and the eating-related psychological traits in eating disorders (anorexia nervosa and bulimia) and obesity. Eat Weight Disord 12:91–96.
14. Stice E, Spoor S, Bohon C, Small DM (2008): Relation between obesity and blunted striatal response to food is moderated by TaqIA A1 allele. Science 322:449–452.

15. Jocham G, Klein TA, Neumann J, von Cramon DY, Reuter M, Ullsperger M (2009): Dopamine DRD2 polymorphism alters reversal learning and associated neural activity. J Neurosci 29:3695–3704.

16. Whitton AE, Treadway MT, Pizzagalli DA (2015): Reward processing dysfunction in major depression, bipolar disorder and schizophrenia. Curr Opin Psychiatry 28:7–12.

17. Ott T, Nieder A (2019): Dopamine and cognitive control in prefrontal cortex. Trends Cogn Sci 23:213–234.

18. Nymberg C, Banaschewski T, Bokde AL, Büchel C, Conrod P, Flor H, et al. (2014): DRD2/ANKK1 polymorphism modulates the effect of ventral striatal activation on working memory performance. Neuropsychopharmacology 39:2357–2365.

19. Berryhill ME, Wiener M, Stephens JA, Lohoff FW, Coslett HB (2013): COMT and ANKK1-Taq-Ia genetic polymorphisms influence visual working memory. PLoS One 8:e55862.

20. Felsted JA, Ren X, Chouinard-Decorte F, Small DM (2010): Genetically determined differences in brain response to a primary food reward. J Neurosci 30:2428–2432.

21. White MJ, Morris CP, Lawford BR, Young RM (2008): Behavioral phenotypes of impulsivity related to the ANKK1 gene are independent of an acute stressor. Behav Brain Funct 4:54.

22. Hamidovic A, Dlugos A, Skol A, Palmer AA, de Wit H (2009): Evaluation of genetic variability in the dopamine receptor D2 in relation to behavioral inhibition and impulsivity/sensation seeking: An exploratory study with d-amphetamine in healthy participants. Exp Clin Psychopharmacol 17:374–383.

23. Jönsson EG, Nöthen MM, Grünhage F, Farde L, Nakashima Y, Propping P, Sedvall GC (1999): Polymorphisms in the dopamine D2 receptor gene and their relationships to striatal dopamine receptor density of healthy volunteers. Mol Psychiatry 4:290–296.

24. Pohjalainen T, Rinne JO, Någren K, Lehikoinen P, Anttila K, Syvälahti EK, Hietala J (1998): The A1 allele of the human D2 dopamine receptor gene predicts low D2 receptor availability in healthy volunteers. Mol Psychiatry 3:256–260.

25. Thompson J, Thomas N, Singleton A, Piggott M, Lloyd S, Perry EK, et al. (1997): D2 dopamine receptor gene (DRD2) Taq1 A polymorphism: Reduced dopamine D2 receptor binding in the human striatum associated with the A1 allele. Pharmacogenetics 7:479–484.

26. Wang GJ, Volkow ND, Logan J, Pappas NR, Wong CT, Zhu W, et al. (2001): Brain dopamine and obesity. Lancet 357:354–357.

27. Johnson PM, Kenny PJ (2010): Dopamine D2 receptors in addiction-like reward dysfunction and compulsive eating in obese rats [published correction appears in Nat Neurosci 2010;13:1033]. Nat Neurosci 13:635–641.

28. Friend DM, Devarakonda K, O'Neal TJ, Skirzewski M, Papazoglou I, Kaplan AR, et al. (2017): Basal ganglia dysfunction contributes to physical inactivity in obesity. Cell Metab 25:312–321.

29. Berland C, Montalban E, Perrin E, Di Miceli M, Nakamura Y, Martinat M, et al. (2020): Circulating triglycerides gate dopamine-associated behaviors through DRD2-expressing neurons. Cell Metab 31:773–790.e11.

30. Berland C, Castel J, Terrasi R, Montalban E, Foppen E, Martin C, et al. (2022): Identification of an endocannabinoid gut-brain vagal mechanism controlling food reward and energy homeostasis. Mol Psychiatry 27:2340–2354.

31. Montalban E, Giralt A, Taing L, Schut EHS, Supiot LF, Castell L, et al. (2022): Translational profiling of mouse dopaminoceptive neurons reveals region-specific gene expression, exon usage, and striatal prostaglandin E2 modulatory effects. Mol Psychiatry 27:2068–2079.

32. Schmidt EF, Kus L, Gong S, Heintz N (2013): BAC transgenic mice and the GENSAT database of engineered mouse strains. Cold Spring Harb Protoc 2013; 2013:pdb.top073692.

33. Zucker RS, Regehr WG (2002): Short-term synaptic plasticity. Annu Rev Physiol 64:355–405.

34. Ducrocq F, Walle R, Contini A, Oummadi A, Caraballo B, van der Veldt S, et al. (2020): Causal link between n-3 polyunsaturated fatty acid deficiency and motivation deficits. Cell Metab 31:755–772.e7.

35. Francis TC, Yano H, Demarest TG, Shen H, Bonci A (2019): High-frequency activation of nucleus accumbens D1-MSNs drives excitatory potentiation on D2-MSNs. Neuron 103:432–444.e3.

36. Oliveira MG, Bueno OF, Pomarico AC, Gugliano EB (1997): Strategies used by hippocampal- and caudate-putamen-lesioned rats in a learning task. Neurobiol Learn Mem 68:32–41.

37. Sala-Bayo J, Fiddian L, Nilsson SRO, Hervig ME, McKenzie C, Mareschi A, et al. (2020): Dorsal and ventral striatal dopamine D1 and D2 receptors differentially modulate distinct phases of serial visual reversal learning. Neuropsychopharmacology 45:736–744.

38. Simpson EH, Balsam PD (2016): The behavioral neuroscience of motivation: An overview of concepts, measures, and translational applications. Curr Top Behav Neurosci 27:1–12.

39. Ter Horst KW, Lammers NM, Trinko R, Opland DM, Figee M, Ackermans MT, et al. (2018): Striatal dopamine regulates systemic glucose metabolism in humans and mice. Sci Transl Med 10:eaar3752.

40. Mullally JA, Chung WK, LeDuc CA, Reid TJ, Febres G, Holleran S, et al. (2021): Weight-loss response to naltrexone/bupropion is modulated by the Taq1A genetic variant near DRD2 (rs1800497): A pilot study. Diabetes Obes Metab 23:850–853.

41. Heni M, Kullmann S, Ahlqvist E, Wagner R, Machicao F, Staiger H, et al. (2016): Interaction between the obesity-risk gene FTO and the dopamine D2 receptor gene ANKK1/TaqIA on insulin sensitivity. Diabetologia 59:2622–2631.

42. Sevgi M, Rigoux L, Kühn AB, Mauer J, Schilbach L, Hess ME, et al. (2015): An obesity-predisposing variant of the FTO gene regulates D2R-dependent reward learning. J Neurosci 35:12584–12592.

43. Denis RG, Joly-Amado A, Cansell C, Castel J, Martinez S, Delbes AS, Luquet S (2014): Central orchestration of peripheral nutrient partitioning and substrate utilization: Implications for the metabolic syndrome. Diabetes Metab 40:191–197.

44. Joly-Amado A, Denis RG, Castel J, Lacombe A, Cansell C, Rouch C, et al. (2012): Hypothalamic AgRP-neurons control peripheral substrate utilization and nutrient partitioning. EMBO J 31:4276–4288.

45. Guegan T, Cutando L, Ayuso E, Santini E, Fisone G, Bosch F, et al. (2013): Operant behavior to obtain palatable food modifies neuronal plasticity in the brain reward circuit. Eur Neuropsychopharmacol 23:146–159.

46. Stelzel C, Basten U, Montag C, Reuter M, Fiebach CJ (2010): Frontostriatal involvement in task switching depends on genetic differences in d2 receptor density. J Neurosci 30:14205–14212.

47. Chaix A, Lin T, Le HD, Chang MW, Panda S (2019): Time-restricted feeding prevents obesity and metabolic syndrome in mice lacking a circadian clock. Cell Metab 29:303–319.e4.

48. Zhao L, Hutchison AT, Liu B, Yates CL, Teong XT, Wittert GA, et al. (2022): Time-restricted eating improves glycemic control and dampens energy-consuming pathways in human adipose tissue. Nutrition 96:111583.

49. Gallo EF, Meszaros J, Sherman JD, Chohan MO, Teboul E, Choi CS, et al. (2018): Accumbens dopamine D2 receptors increase motivation by decreasing inhibitory transmission to the ventral pallidum. Nat Commun 9:1086.

50. Trifilieff P, Feng B, Urizar E, Winiger V, Ward RD, Taylor KM, et al. (2013): Increasing dopamine D2 receptor expression in the adult nucleus accumbens enhances motivation. Mol Psychiatry 18:1025–1033.

51. Hernandez L, Hoebel BG (1988): Food reward and cocaine increase extracellular dopamine in the nucleus accumbens as measured by microdialysis. Life Sci 42:1705–1712.

52. Chersi F, Burgess N (2015): The cognitive architecture of spatial navigation: Hippocampal and striatal contributions. Neuron 88:64–77.

53. Floresco SB, Ghods-Sharifi S, Vexelman C, Magyar O (2006): Dissociable roles for the nucleus accumbens core and shell in regulating set shifting. J Neurosci 26:2449–2457.

54. Verharen JPH, de Jong JW, Roelofs TJM, Huffels CFM, van Zessen R, Luijendijk MCM, et al. (2018): A neuronal mechanism underlying decision-making deficits during hyperdopaminergic states. Nat Commun 9:731.

55. Macpherson T, Morita M, Wang Y, Sasaoka T, Sawa A, Hikida T (2016): Nucleus accumbens dopamine D2-receptor expressing

neurons control behavioral flexibility in a place discrimination task in the IntelliCage. Learn Mem 23:359–364.

56. Noonan MA, Bulin SE, Fuller DC, Eisch AJ (2010): Reduction of adult hippocampal neurogenesis confers vulnerability in an animal model of cocaine addiction. J Neurosci 30:304–315.

57. Dalley JW, Fryer TD, Brichard L, Robinson ESJ, Theobald DEH, Lääne K, et al. (2007): Nucleus accumbens D2/3 receptors predict trait impulsivity and cocaine reinforcement. Science 315:1267–1270.

58. Gullo MJ, St John N, McD Young R, Saunders JB, Noble EP, Connor JP (2014): Impulsivity-related cognition in alcohol dependence: Is it moderated by DRD2/ANKK1 gene status and executive dysfunction? Addict Behav 39:1663–1669.

59. Eisenberg DT, Mackillop J, Modi M, Beauchemin J, Dang D, Lisman SA, et al. (2007): Examining impulsivity as an endophenotype using a behavioral approach: A DRD2 TaqI A and DRD4 48-bp VNTR association study. Behav Brain Funct 3:2.

60. Klein TA, Neumann J, Reuter M, Hennig J, von Cramon DY, Ullsperger M (2007): Genetically determined differences in learning from errors. Science 318:1642–1645.

61. Coppin G, Nolan-Poupart S, Jones-Gotman M, Small DM (2014): Working memory and reward association learning impairments in obesity. Neuropsychologia 65:146–155.

62. Lee JC, Mueller KL, Tomblin JB (2016): Examining procedural learning and corticostriatal pathways for individual differences in language: Testing endophenotypes of DRD2/ANKK1. Lang Cogn Neurosci 31:1098–1114.

63. Sun X, Luquet S, Small DM (2017): DRD2: Bridging the genome and ingestive behavior. Trends Cogn Sci 21:372–384.

64. Labouesse MA, Sartori AM, Weinmann O, Simpson EH, Kellendonk C, Weber-Stadlbauer U (2018): Striatal dopamine 2 receptor upregulation during development predisposes to diet-induced obesity by reducing energy output in mice. Proc Natl Acad Sci U S A 115:10493–10498.

65. Wagner A, Aizenstein H, Venkatraman VK, Fudge J, May JC, Mazurkewicz L, et al. (2007): Altered reward processing in women recovered from anorexia nervosa. Am J Psychiatry 164:1842–1849.

66. Guo J, Simmons WK, Herscovitch P, Martin A, Hall KD (2014): Striatal dopamine D2-like receptor correlation patterns with human obesity and opportunistic eating behavior [published correction appears in Mol Psychiatry 2022;27:4369]. Mol Psychiatry 19:1078–1084.

67. South T, Huang XF (2008): High-fat diet exposure increases dopamine D2 receptor and decreases dopamine transporter receptor binding density in the nucleus accumbens and caudate putamen of mice. Neurochem Res 33:598–605.

68. Huang W, Payne TJ, Ma JZ, Beuten J, Dupont RT, Inohara N, Li MD (2009): Significant association of ANKK1 and detection of a functional polymorphism with nicotine dependence in an African-American sample. Neuropsychopharmacology 34:319–330.

69. Bontempi S, Fiorentini C, Busi C, Guerra N, Spano P, Missale C (2007): Identification and characterization of two nuclear factor-kappaB sites in the regulatory region of the dopamine D2 receptor. Endocrinology 148:2563–2570.